Geomorphology 432 (2023) 108705

Contents lists available at ScienceDirect

Geomorphology

journal homepage: www.journals.elsevier.com/geomorphology

Meandering river evolution in an unvegetated permafrost environment

Joseph S. Levy *, Bronson Cvijanovich

Colgate University Dept. of Earth and Environmental Geosciences, Hamilton, NY 13346, USA

ARTICLE INFO

Keywords:
Fluvial
Permafrost
Meander
Point bar
Antarctica

ABSTRACT

Meandering river sedimentary facies are associated with the rise of terrestrial vegetation in the rock record, but modern examples of highly sinuous, single-threaded streams are also found in many modern non-vegetated environments. Prior workers have speculated that permafrost or ice-cemented sediment could provide the cohesion needed to generate single-threaded, meandering channels, however, the presence of bank vegetation in the overwhelming majority of terrestrial permafrost sites in which meandering rivers are present has made it impossible to disentangle the relative impact of bank cohesion provided by frozen sediments from that provided by roots. Here, we examine topographic change over 13 years at the Onyx River, an unvegetated, permafrost-affected, sand-and-gravel-bottomed river in the McMurdo Dry Valleys (MDV) of Antarctica, supported by ~40 years of image data. On the basis of lidar change detection and satellite/airborne image analysis, we find that meandering river processes (cut bank erosion, point bar growth, and meander migration) can occur in this ice-cemented, unvegetated permafrost river system. We find that the Onyx River's upper, single-threaded reach is meandering, and that bank cohesion is provided by ice-cemented permafrost. Meander migration rates within the Onyx's meandering reach are extremely close to values predicted based on observations of meander migration rates in other unvegetated rivers, however, the short (~70 day) duration of Onyx River discharge suggests these migration rates should be considered low estimates, which could be up to ~5 times greater during the short, summer erosion season. Together, these observations suggest that ice-cemented permafrost is a weak form of bank cohesion that can result in rapid landscape change in response to thermokarstic fluvial erosion, producing dynamic river channels, especially where warm meltwater encounters ice-rich permafrost deposits.

1. Introduction

River channel morphology reflects the interplay between hydrological and climate forcing and geological and sedimentary landscape response. While the adjustment of river channels towards equilibrium conditions can occur over years to decades in some rapidly evolving reaches (Church and Ferguson, 2015; Naito and Parker, 2020), river channel morphology most commonly is interpreted as a result of long-term processes related to sediment supply, discharge, and landscape properties (e.g., Lane and Richards, 1997). This is particularly true when fluvial sediment deposits are considered in the rock record; because meandering river sedimentary facies are associated with the rise of terrestrial vegetation (Davies and Gibling, 2010; Ielpi et al., 2022; Schumm, 1968), the appearance of these deposits is interpreted to mark a step change in terrestrial surface processes.

However, modern examples of highly sinuous, meandering, single-threaded streams are also found in many modern non-vegetated environments in which other processes generate bank cohesion (Lapôtre et al., 2019). For example, calcium-sulfate-bonded banks generate meandering rivers in the Atacama (Ritter et al., 2022) and clays can bond temperate, arid-climate stream banks (Matsubara et al., 2015). Marine sediments can provide bank cohesion to generate meandering channels on submarine fan systems (Babonneau et al., 2010; Clark et al., 1992), while high-sinuosity channel forms can grow atop nearly sediment-free glacier ice (Karlstrom et al., 2013). These studies raise the question of what other sedimentary processes can provide bank cohesion to give rise to meandering rivers, and how the presence of meandering river sedimentary facies should be interpreted to inform paleoclimate processes at work in ancient river basins.

The detection of sedimentary deposits on Mars that are inferred to have formed as a result of sediment transport in meandering rivers raises the question of what process or processes could provide cohesion in martian regolith to allow single-threaded channels to form and evolve (Cardenas et al., 2018; Fassett and Head, 2005; Goudge et al., 2016;

* Corresponding author.
E-mail address: jlevy@colgate.edu (J.S. Levy).

https://doi.org/10.1016/j.geomorph.2023.108705
Received 16 January 2023; Received in revised form 26 March 2023; Accepted 12 April 2023
Available online 17 April 2023

Howard, 2009; Lapôtre and Ielpi, 2020; Matsubara et al., 2015; Weihaupt, 1974). Given cold climate conditions that persisted during much of the Noachian (Fairén, 2010; Wordsworth, 2016; Wordsworth et al., 2015), prior workers have speculated that permafrost or ice-cemented sediment could provide the cohesion needed to generate single-threaded, meandering channels, however, the presence of bank vegetation in the overwhelming majority of terrestrial permafrost sites in which meandering rivers are present has made it impossible to disentangle the relative impact of bank cohesion provided by frozen sediments from that provided by roots (Matsubara et al., 2015).

Indeed, while Arctic meandering rivers show a wide range of meander migration rates, from as low as 0.5 m/yr on the Yukon River (Douglas et al., 2022), to as high as 10s of m/year on the subaerial portions of arctic deltas (Jarriel et al., 2021), vegetation plays a dominant role in determining meander migration rates, even in these permafrost-affected environments. Ielpi et al. (2023) found a systematic decrease in Arctic river meander migration rates, from ~6.8 m/yr in 1980 to ~5.2 in 2020, which they showed resulted primarily from bank shrubification, and secondarily, from enhanced infiltration into thawing permafrost. The importance of bank vegetation in shaping Arctic permafrost-affected rivers strongly motivates the need to identify a location in which meandering river processes can be evaluated in the presence of permafrost, but in the absence of vascular land plants.

Here, we examine topographic change over 13 years at the Onyx River, an unvegetated, permafrost-affected, sand-and-gravel-bottomed river in the McMurdo Dry Valleys (MDV) of Antarctica, supported by ~40 years of image data. Our goals are to determine: 1) are meandering river sedimentary processes occurring (e.g., cut bank migration and point bar growth), 2) what is the rate of meander migration for an unvegetated, ice-cemented, sediment-floored channel, 3) what is the sediment budget of the Onyx River within each distinct reach and as a whole, and 4) what does fluvial sediment transport and deposition in a glacier-fed, permafrost-dominated, unvegetated stream channel on Earth suggest about the interpretation of meandering river deposits on Mars.

2. Regional setting

The Onyx River is the longest subaerial, sediment-bedded river in Antarctica (Fig. 1). It rises near −77.43°N, 162.73°E, flowing out of Lake Brownworth, a proglacial lake at the toe of Lower Wright Glacier, and flows ~32 km (Shaw and Healy, 1980) west to its terminus at Lake Vanda. The Onyx flows through Wright Valley, one of the McMurdo Dry Valleys (MDV), which have a mean annual air temperature near −18 °C (Doran et al., 2002) and are devoid of vascular plants. The typical discharge season for the Onyx River is November 30 to February 7, peaking near January 1, with an average total annual discharge of ~3 × 10^6 m^3 (Gooseff et al., 2007; Wlostowski et al., 2016). The Onyx flows only during Antarctic summer. Peak discharge conditions are associated with warm air temperatures and clear skies that optimize insolation and sensible heat flux (Chinn and Mason, 2016; Gooseff et al., 2007; Shaw and Healy, 1980). The daily hydrograph is controlled largely by solar illumination azimuth, peaking after the insolation maximum on the west-facing Lower Wright Glacier (Shaw and Healy, 1980), similar to other glacier-fed streams in the MDV which show solar azimuth control over glacier runoff generation (Conovitz et al., 1998).

On the basis of field observations and aerial imaging, Shaw and Healy (1980) identified three major reach classes for the Onyx: an upper sinuous/meandering section, a lower alluvial/braided section, and a terminal section where discharge is largely over exposed bedrock and between large boulders. The stream bed and bank terraces are sand and gravel dominated, with mean terrace grain size spanning Φ = −3 to −5 (8 mm to 32 mm), and mean channel bed material spanning Φ = 1 to −5 (0.5 mm to 32 mm), dominated by Φ = 0–1 (0.5–1 mm) grains but with coarser armoring sediment present (Shaw and Healy, 1980). On the basis of airborne lidar measurements collected in 2014–2015, Levy et al. (2018) identified potential sites of cut bank incision on the Onyx, consistent with prior airborne and ground-based geomorphic work from Shaw and Healy (1980) that described a range of bar and terrace morphologies. For example, Shaw and Healy (1980) infer a three-regime model to explain the origin of point bars observed in the Onyx involving: 1) aggradation of point bar sediments during periods of low flow, 2) subequal aggradation of point bars and erosion of cut bank sediments at intermediate discharge, and 3) bank erosion that greatly exceeds point bar accumulation at high flow, leading to transitional deposits interpreted as longitudinal bars. Together, these observations point towards the Onyx being a strong candidate for identification of meandering river processes and deposits in a permafrost setting.

Permafrost is continuous in Wright Valley. In the Onyx River basin, permafrost is largely ice-cemented (Bockheim et al., 2007) but also includes ice-cored moraines and other buried ice deposits (Levy et al., 2018). Active layer thicknesses average 20–45 cm on stream bank terraces and rise to up to 75 cm in the immediate vicinity of the stream channel (Bockheim et al., 2007). Thermal contraction crack polygons are common in Wright Valley (Black, 1982) and cover valley wall and Onyx River terrace surfaces, providing evidence of continuous permafrost conditions over millennial timescales (Sletten et al., 2003).

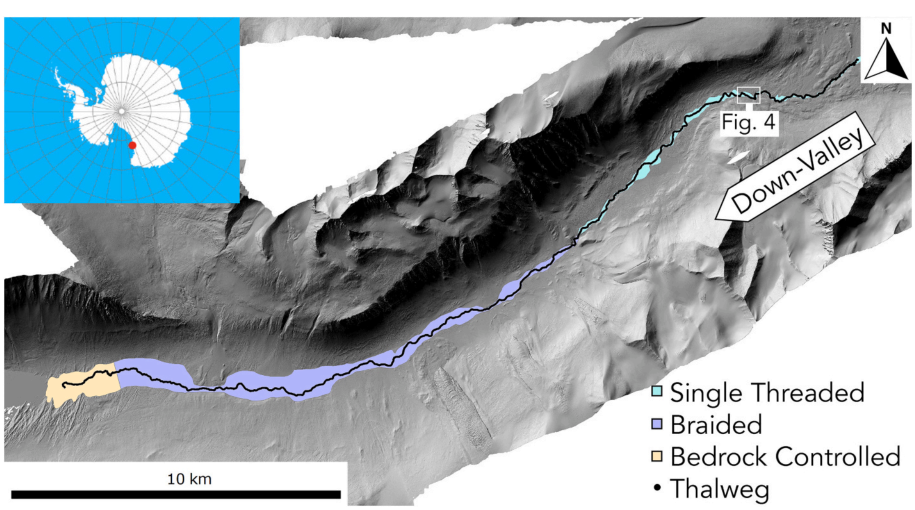

Fig. 1. The Onyx River regional setting. The Onyx River is located in Wright Valley, Antarctica, and flows from east to west (right to left), from the Lower Wright Glacier to Lake Vanda. The river has three main reach morphologies—a single-channel upper reach, a braided intermediate reach, and a terminal reach characterized by flow over bedrock and/or boulders. Inset map shows location of the McMurdo Dry Valleys (MDV) in Antarctica. Inset map grid is 10° latitude and longitude.

3. Methods

Lidar point cloud data collected in 2001 (Csatho et al., 2005) and 2014 (Fountain et al., 2017) form the basis for change analysis. The Onyx River was manually divided into the major reach sections on the basis of channel morphology (single thread, braided, or bedrock/boulder-controlled) after Shaw and Healy (1980), using the Fountain et al., (2017) 1 m/pixel lidar hillshade supported by Worldview satellite image data where needed to disambiguate channel location or to determine if a channel segment was active. The Onyx thalweg was computed using the AcrGIS Hydrology toolset and manually pruning tributary branches or channels until only the lowest valley thalweg remained. Elevation from the Fountain et al. (2017) 1 m/pixel digital elevation model (DEM) was sampled every meter along the thalweg to determine channel elevation, slope (rise/run between upstream and downstream elevation points), and sinuosity over a 500 m moving window reach length (i.e., channel length divided by straight-line distance between the beginning and end point of the moving window) (Fig. 2).

The 2001 and 2014 point cloud datasets were processed into a triangulated irregular network (TIN) to enable change detection. The 2001 and 2014 TINs were differenced, and the resulting change TIN was gridded into a 1 m/pixel DEM of difference, taking the average TIN elevation change within each cell. The DEM of difference convention used in this study is that negative values indicate surface lowering from 2001 to 2014 and positive values indicate elevation gain. The RMSE for the distance-to-plane measurement in the 2014 lidar is 7.6 cm, with a vertical and horizontal component RMSE of 6.9 and 3.2 cm, respectively (Fountain et al., 2017)—on the spatial scale of the 1 m/pixel DEM of differences, the 7.6 cm vertical uncertainty dominates pixel elevation uncertainty and is used as the basis for determining volume change uncertainty. To account for uncertainty derived from the 2001 and 2014 kinematic surveys, as well as different lidar scan patterns, flight orientations and aircraft dynamics, etc., we adopt a conservative minimum change detection threshold of ±25 cm (after Fountain et al., 2017; and Levy et al., 2018), filtering out pixels from the DEM of difference that do not exceed this threshold.

In order to evaluate the dominance of the meandering channel processes, a comparison of the morphology of different channel sections was performed. Elevation change (and therefore volume change) along the entire active alluvial level was calculated for each reach segment. The positions of 30 cut bank and point bar pairs were identified in the 2001 and 2014 DEM hillshades. Volume change within the footprint of the point bar and cut bank was determined for each pair using the DEM of difference. In addition, cut bank traces identified in each DEM hillshade were manually digitized in order to determine migration distance between lidar data collections. In order to evaluate migration rates, Onyx River channel widths were measured from Worldview satellite image data (image WV01_20161218234542_102001005C18BF00_16DEC18234542 collected on 18 December 2016, ~0.6 m/pixel) upstream and downstream of each cut bank pair. Image data was used to measure channel width because it is higher spatial resolution than the 1 m/pixel lidar and because contrast between bright sediment and dark water is more apparent in image data than in lidar, allowing for sharp determination of channel boundaries. Finally, satellite image data and air photos were inspected to determine the presence or absence of sand-wedge thermal contraction crack polygon fracture growth on point bars as an indicator of permafrost aggradation through newly formed point bar deposits. These imaging datasets were collected in 1983 (US Navy TMA air photo collection) and 2018 (Worldview satellite image data, courtesy Polar Geospatial Center), which bracket the period of lidar data collection. The TMA images were selected due to their exceptionally high clarity in comparison with image data collected concurrently with the 2001–2 airborne lidar campaign. The Worldview image was selected on the basis of clear image lighting and feature contrast, as well as collection time within the December–January seasonal timeframe during which both lidar datasets were collected.

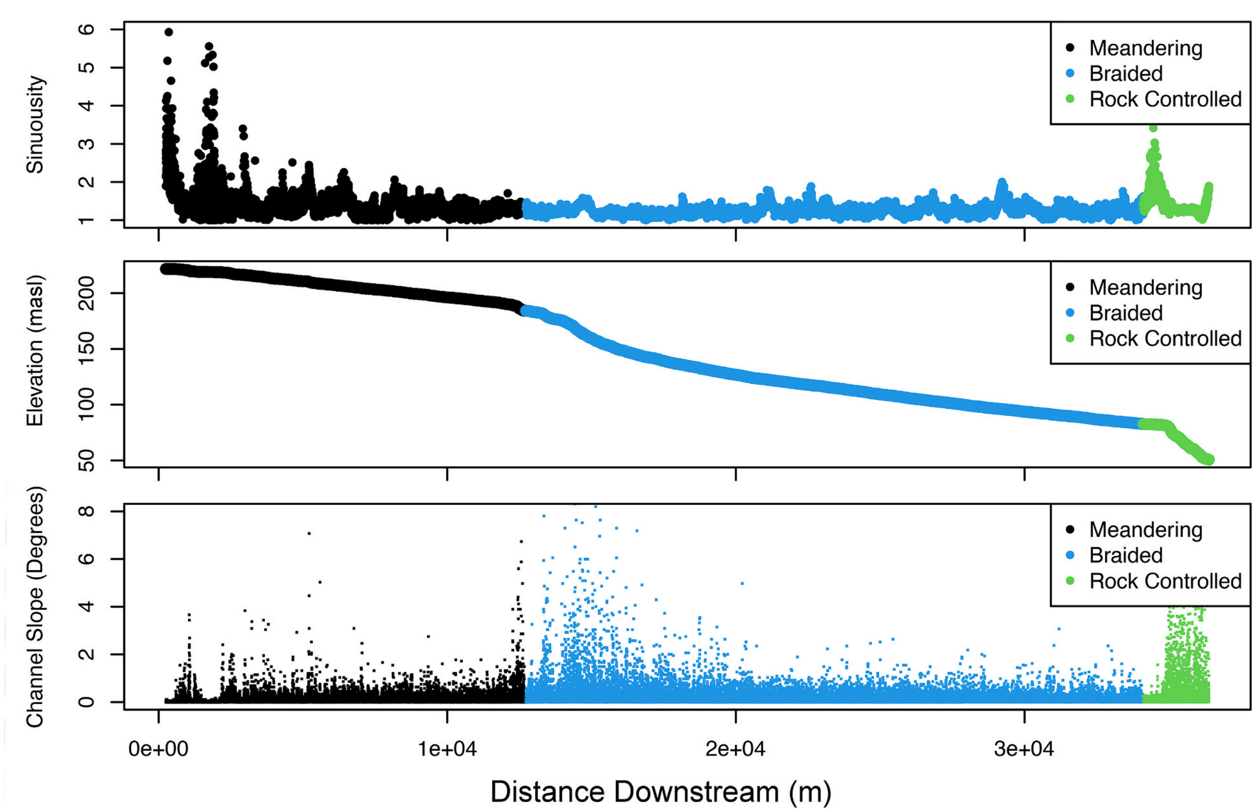

Fig. 2. Onyx River thalweg profiles of slope, elevation, and sinuosity. The Onyx can be divided into three major reach classes on the basis of channel morphology: a high sinuosity, high elevation, low slope meandering reach; a low sinuosity, high-slope braided reach, and a terminal bedrock and boulder-controlled reach.

4. Results

The Onyx River can be divided into three major reach classes on the basis of thalweg characteristics (sinuosity, elevation, and slope), which recapitulate the morphological reach classes proposed by Shaw and Healy (1980) (Fig. 2). On the basis of thalweg characteristics, the upper, meandering reach has sinuosity values typically >2, and up to ~6, a low slope of 10^{-5} m/m, and an area of 1.47×10^6 m^2. The intermediate braided reach is steeper, has a lower sinuosity than the meandering reach, and has an area of 7.62×10^6 m^2. The bedrock and boulder controlled reach at the mouth of the Onyx River at Lake Vanda is the steepest reach, has an area of 1.83×10^6 m^2, and due to curvature of the channel and short-wavelength diversions between and around boulders also shows high sinuosity.

Analysis of the position of thirty cut banks showed bank displacements from 3.0 to 39.9 m over the period 2001 to 2014. This corresponds to an average migration rate (Mr) of 0.2 to 3.1 m/yr, with an average rate of 1.4 m/yr across all cut banks (Fig. 3). These cut bank migration rates occurred in proximity to channel widths spanning 3.5 to 14.3 m, with an average channel width of 8.6 m, based on 48 measurements immediately upslope and downslope of cut bank sites on a Worldview 1 image collected 12/18/16 (Image WV01_20161218234542).

Elevation change detected in the DEM of difference is localized to specific regions of the Onyx River channel system. Subsidence in the meandering region is dominated by bank cutting and aggradation is concentrated at point bars (Fig. 4). At most cut bank-point bar pairs, cut bank erosion exceeds point bar aggradation, however, at approximately 1/3 of pairs, deposition along the point bar exceeds cut bank erosion (Fig. 5).

Lidar change detection reveals spatial patterns within the sediment budget of the Onyx River at the reach scale. Subsidence in the meandering region is dominated by bank cutting, while subsidence in the braided region is dominated by terrace incision and bar movement (Fig. 6). Aggradation in the meandering reach is largely localized at point bars, while in the braided region, aggradation is concentrated within channels.

At the reach scale, the Onyx River sediment budget is mostly in equilibrium within the meandering reach and is accumulating sediment in the braided reach. Net volume change in the meandering reach from 2001 to 2014 was $-5200 \pm 18{,}000$ m^3, while net volume change in the braided reach was $+311{,}000 \pm 85{,}600$ m^3 (Fig. 7). Breaking down the net change values, subsidence in meandering reach was much greater than in the braided reach due to laterally extensive pockets of thick (several meter tall) cut bank erosion in the meandering reach, versus thinner terrace and channel cuts in the braided reach. Despite the braided reach having a considerably larger area than the meandering reach, erosion in the meandering reach was $-62{,}000 \pm 5600$ m^3 (~84 cm subsidence for pixels showing subsidence exceeding lidar measurement uncertainty) versus subsidence in the braided reach of only $-41{,}600 \pm 7100$ m^3 (~45 cm subsidence for pixels showing subsidence exceeding lidar measurement uncertainty). Point bar deposition in the meandering reach led to sediment accumulation in this region close to balancing erosion, $+57{,}000 \pm 12{,}400$ m^3 (~35 cm aggradation for pixels showing elevation gain exceeding lidar uncertainty), while channel fills in the braided reach led to widespread accumulation of sediment totaling $+352{,}000 \pm 78{,}500$ m^3 (~34 cm aggradation for pixels showing elevation gain exceeding lidar uncertainty). Aggradation dispersed across the terminal bedrock controlled reach was $48{,}400 \pm 10{,}500$ m^3 and erosion was $14{,}100 \pm 3000$ m^3 for a net change of $+34{,}300 \pm 13{,}600$ m^3

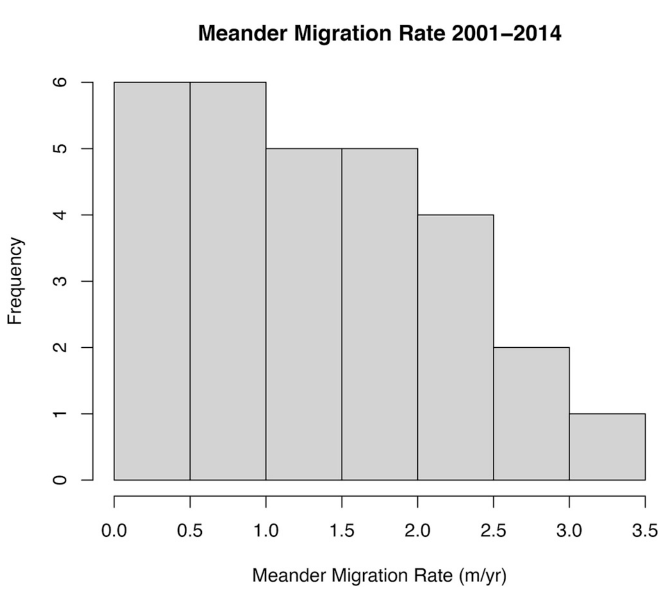

Fig. 3. Meander migration rates. From 2001 to 2014, cut bank locations moved ~1.4 m/yr on average, with peak migration rates approaching 3.1 m/yr.

5. Discussion

This channel morphology change study strongly supports the hypothesis that meandering channels can form in unvegetated, permafrost-affected sand and gravel bedded rivers. The Onyx River shows clear examples of both cut bank incision and paired point bar deposition over inter-annual to decadal timescales. Importantly, ice rather than vegetation is providing bank cohesion in this setting. In the Onyx River system, both the cut banks and point bars show evidence of permafrost presence in the form of sand wedge thermal contraction crack polygons. Importantly, these polygons are cementing not just the intact banks and terraces surrounding the Onyx channel; they are also growing within point bar sediments as epigenetic sand wedges—thermal contraction cracks that are growing up and through the aggrading sediments, suggesting the presence of underlying and aggrading ice-cemented sediment (Fig. 8). This argues that even as thermophysical erosion is removing sediment along the cut bank, aggradation of sediment on the point bar coupled with hyporheic zone wicking (McKnight et al., 1999) are re-cementing point bars with ice-cemented permafrost, providing channel stability on the inner channel curve.

Are meandering channels expected to develop in this setting? The low slopes (~2×10^{-5} median grade in the meandering reach) and coarse grain sizes (sand, granules, and gravel) would generally put the Onyx River near a field of no expected bank erosion in the Lapôtre et al. (2019) meander stability model. However, the fairly low width-to-depth ratios typical of the Onyx River's meandering reach would tend to push the channel closer to meandering conditions and away from braided morphologies, even at these coarse grain sizes (Lapôtre et al., 2019). In the braided portion of the Onyx, typical channel width is approximately 8.6 m and typical flow depth at the Lake Brownworth gage is ~50 cm (Chinn and Mason, 2016; Gooseff et al., 2007; Wlostowski et al., 2016), producing a W/d ratio of ~17.

While meander formation is only marginally predicted under the flow, geometry, and grain size conditions currently characterizing the Onyx River's meandering reach, it is notable that meander migration rates measured in this study compare favorably to empirical models of migration rates based on other, non-vegetated meandering river systems (Ielpi and Lapôtre, 2020). We compare measured meander migration rates on the Onyx River to the empirical meander migration rate relationship from (Ielpi and Lapôtre, 2020) for unvegetated channels:

$$Mr_{unvegetated} = (0.13 \pm 0.02) \cdot w^{(0.84+0.08)} \quad (1)$$

where Mr is meander migration rate (m/year) and w is channel width. Based on our measured channel widths of 3.5 to 14.3 m (mean = 8.6 m),

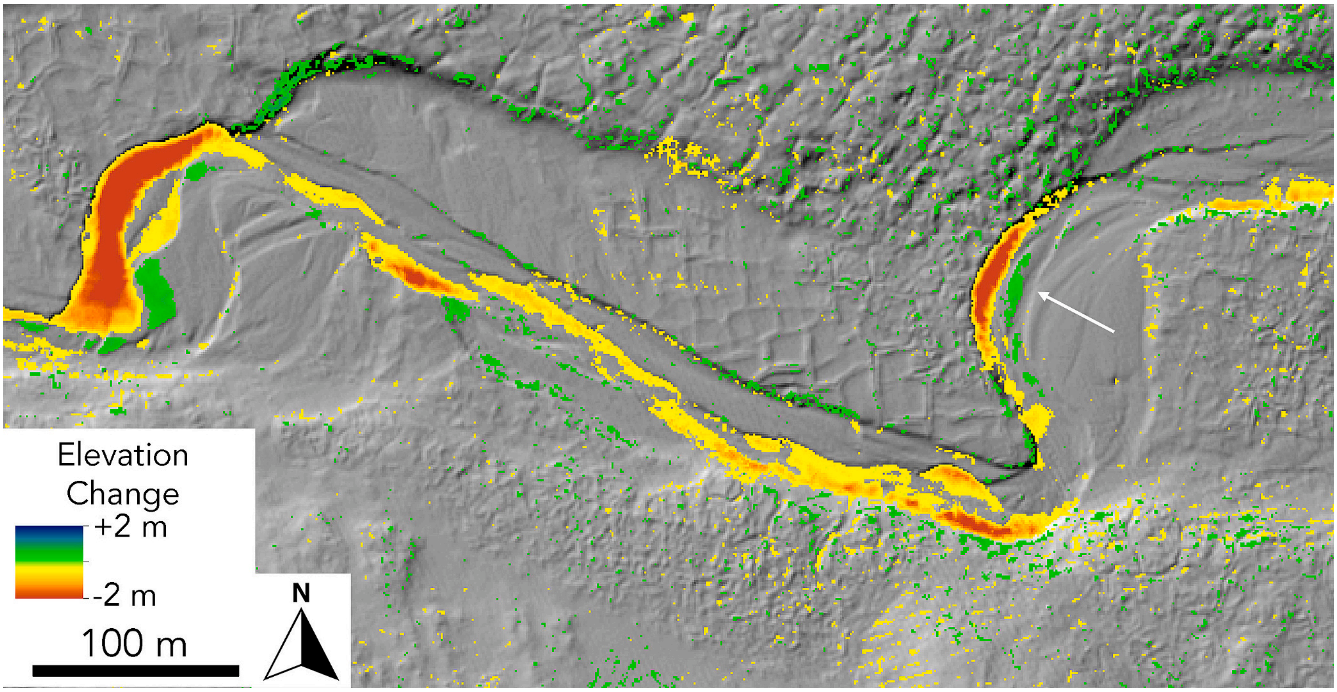

Fig. 4. Example elevation change in the meandering reach. Warm colors (yellow to red) indicate subsidence, cool colors (green to blue) indicate aggradation. Gray pixels showing underlying hillshade indicate surface change of less than ±25 cm. Downstream is to the left. Subsidence is concentrated at cut banks near points of maximum channel curvature. Aggradation is localized along point bars (e.g., white arrow). Bank and terrace material are ice cemented as shown by the presence of thermal contraction crack polygons (sand wedges) at image center. (For interpretation of the references to color in this figure legend, the reader is referred to the web version of this article.)

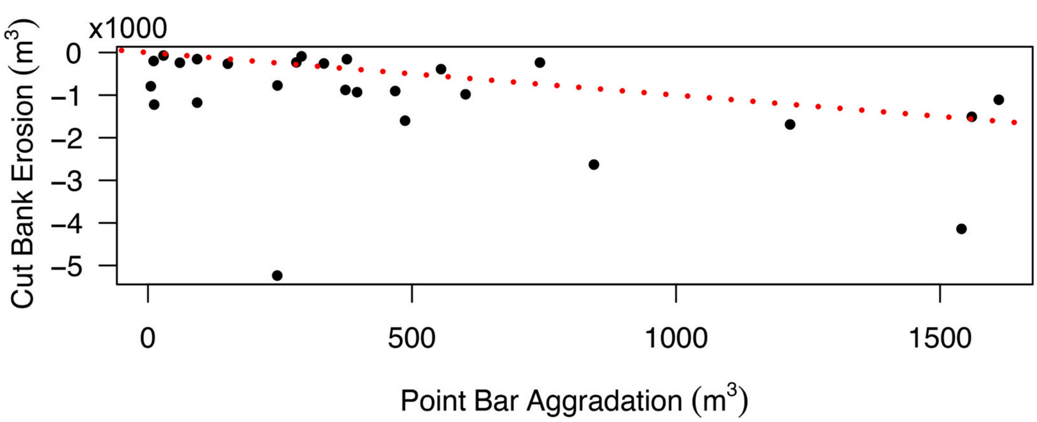

Fig. 5. Aggradation and erosion on point bars and cut banks. At most sites, cut bank erosion exceeds point bar aggradation, however, at approximately 1/3 of meander bends, aggradation of the point bar exceeds cut bank erosion. Red dashed line marks 1:1. (For interpretation of the references to color in this figure legend, the reader is referred to the web version of this article.)

this model produces expected meander migration rates spanning 0.5 to 2 m/yr (mean of 1.1 m/yr). These values largely overlap the observed meander migration rates of 0.2 to 3.1 m/yr, with an average rate of 1.4 m/yr across all cut banks. One possibility is that the highest meander migration rates potentially reflect erosion from higher peak discharge than that observed during typical December discharge conditions.

It is notable that the Ielpi and Lapôtre (2020) relationship so closely matches the meander migration rate on the Onyx River because the Onyx is a highly seasonal river with a very short flow season. In contrast to similarly-sized channels with more continuous (if seasonally modulated) discharge, the Onyx may be eroding its banks faster than would be predicted based on scaling relationships from non-polar environments. One simplistic approach to estimating the erosion rate enhancement is to consider that the Onyx River typically only flows ~70 days/year, between November 30 and February 7 (Gooseff et al., 2007; Wlostowski et al., 2016). Accordingly, meander migration rates could potentially be up to ~5 times greater on the Onyx River than for comparably sized rivers that experience continuous (or at least less strongly episodic) flow.

This accelerated rate of meander migration is consistent with the presence of ice-cored moraine material in the meandering reach of the Onyx River (Levy et al., 2018; Shaw and Healy, 1980). Fluvial bank cutting can accelerate thermokarst subsidence and erosion in polar environments, leading to rapid undercutting and melting of permafrost affected cut banks (Gooseff et al., 2011; Murton, 2009; Sudman et al., 2017; Zhang et al., 2022). Where ice-cored sediments are cross-cut by the Onyx River, rapid thinning or collapse of the cut banks may occur, leading to meander migration rates that could be notably faster than those occurring in warm, unvegetated meandering river environments.

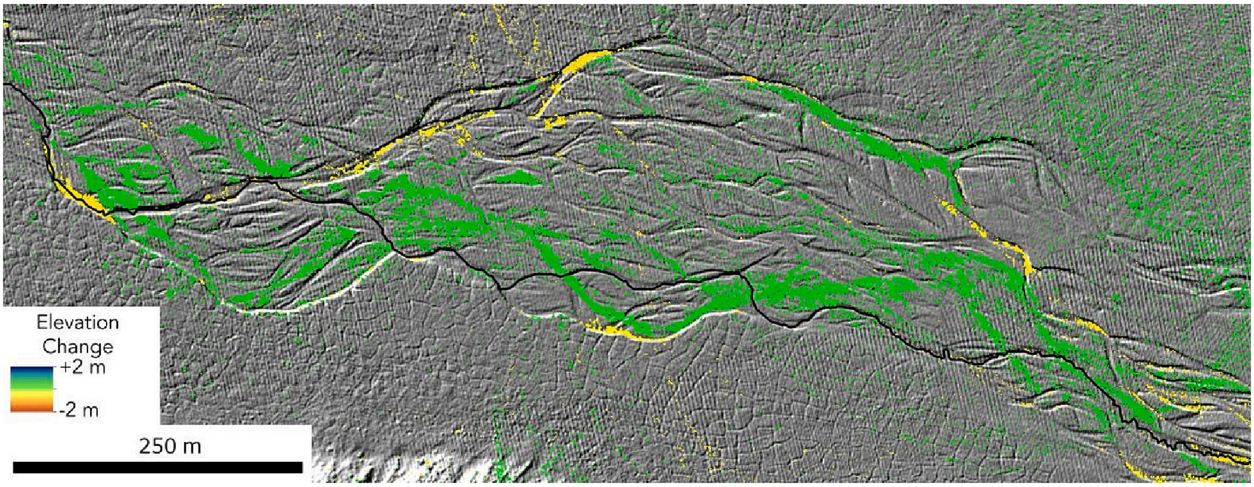

Fig. 6. Surface change in the braided reach. Downslope is to the left. Erosion in the braided reach is primarily terrace cutting and channel incision. Deposition is concentrated in braided channels. The braided region of the Onyx River also has ice-cemented banks, as evidence by thermal contraction crack polygons on terrace surfaces (top and bottom of image). Black line marks current valley thalweg.

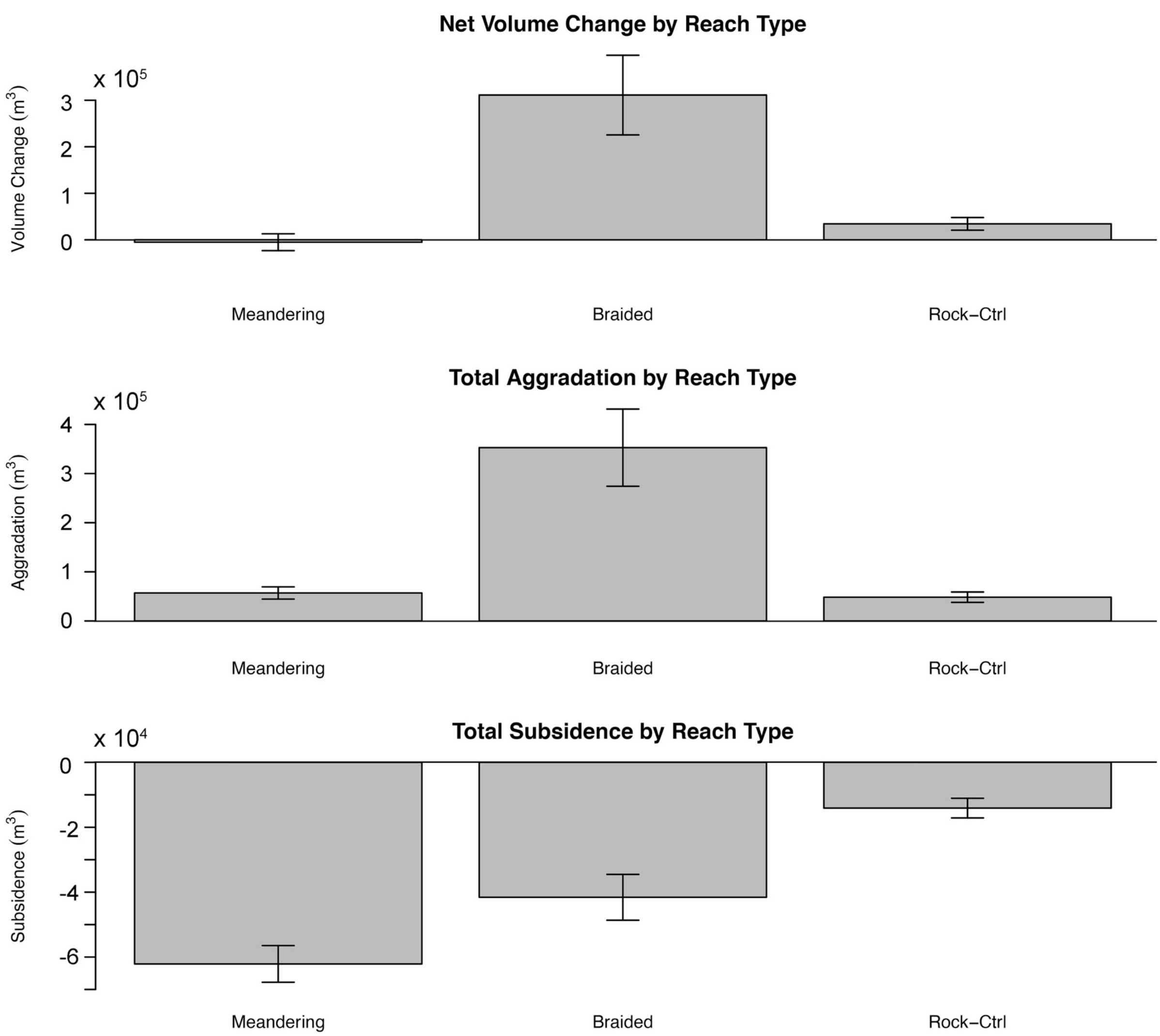

Fig. 7. Reach-scale sediment budget for the Onyx River. The braided reach largely accumulated sediment, while the meandering reach is close to equilibrium and/or is exporting sediment downstream. Despite having a much smaller spatial extent, subsidence in the meandering reach notably exceeds subsidence in the braided reach. The terminal bedrock controlled reach shows net aggradation, but less than in the braided reach.

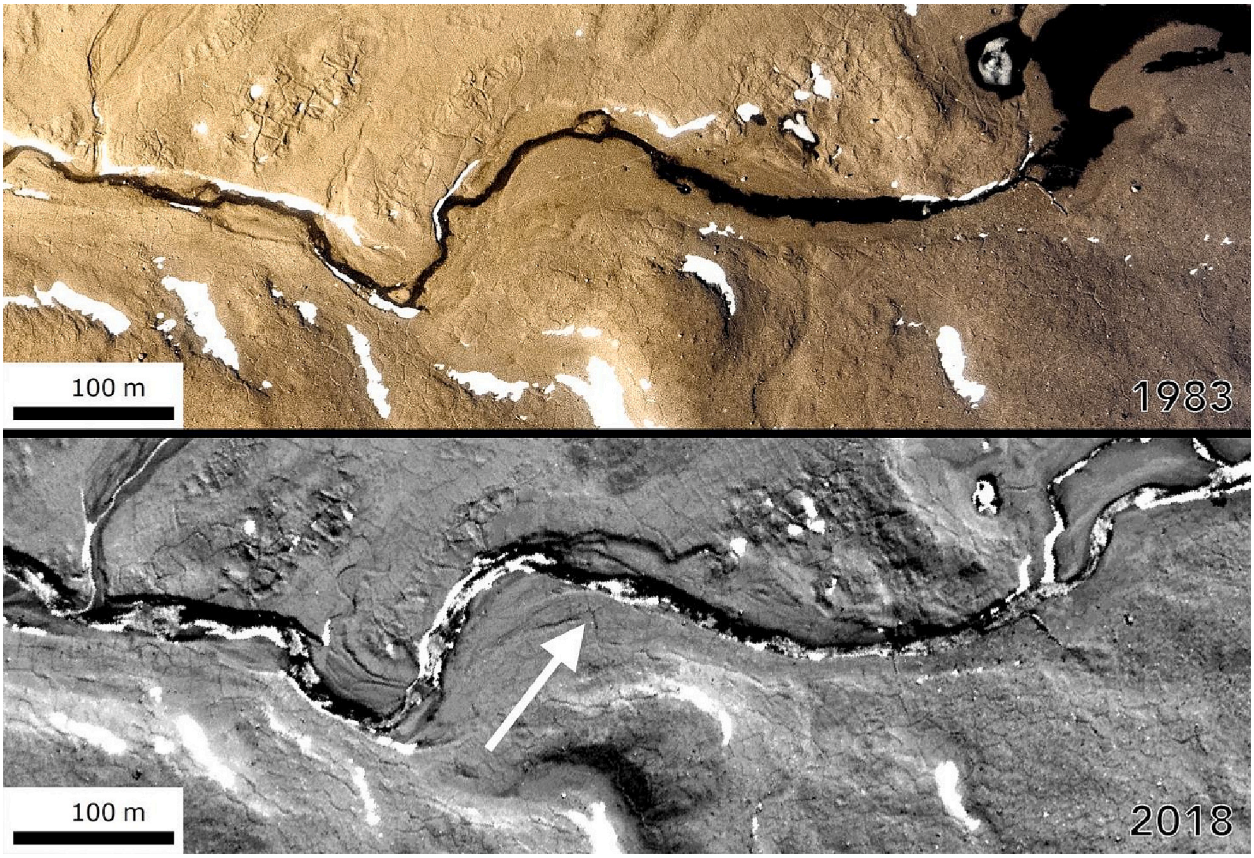

Fig. 8. Epigenetic sand wedge polygons on an Onyx River point bar. Above, air photo from 12-14-1983 (TMA image CA268700V0038); below panchromatic Worldview 1 image collected on 12-16-2018. White arrow shows sand wedge polygon troughs cross-cutting the point bar, suggesting continued presence of permafrost beneath the point bar sediment and re-expansion of sand wedges to crosscut fluvially-deposited sediment.

In the nearby Garwood Valley (one of the southernmost MDV), fluvial thermokarst along the Garwood River has resulted in cut bank erosion rates up to 10 times the Holocene average (up to ~11,000 m^3/year) where fluvial erosion is incising into glacial ice deposits buried beneath thin sedimentary lags (Levy et al., 2013). Such rapid rates of meander migration may depend in part on the presence of buried ice-rich deposits and may represent transitory peaks in erosion rate and meander migration rate. As buried ice deposits are eroded and replaced with more stable, ice-cemented point bar and/or floodplain material, migration rates may slow.

What does the detection and characterization of meandering river structures in an unvegetated permafrost environment in Antarctica mean for interpreting deposits inferred to result from meandering river processes in other cold, dry environments, for example, on Mars? First, these results show unequivocally that meandering river processes can occur in sand and gravel bedded rivers for which bank cohesion is provided entirely by ice-cemented permafrost—not by vegetation, salt cements, or fine-grained sediments. Sedimentary deposits on Mars that are inferred to have formed from meandering river processes (e.g., Cardenas et al., 2018; Fassett and Head, 2005; Goudge et al., 2016; Howard, 2009; Matsubara et al., 2015; Weihaupt, 1974) should be considered candidates for formation under permafrost conditions, and may preserve fluvial permafrost-related facies such as relict sand-wedges resulting from epigenetic growth of sand-wedges as permafrost re-aggrades through point bars. Based on comparisons to terrestrial modeling and scaling studies, meanders in ice-cemented permafrost rivers appear to form even at lower slopes and coarser grain sizes than anticipated, and may migrate up to five times faster when corrected for the short flow season. Together, these observations suggest that ice-cemented permafrost is a weak form of bank cohesion that can generate large geomorphic changes in response to thermo-fluvial erosion. Accordingly, fluvial systems in the rock record on Mars may reflect shorter-lived, more rapidly-changing systems than would otherwise be interpreted based on comparison with warm-climate meandering river systems.

6. Conclusions

On the basis of lidar change detection and satellite/airborne image analysis, we find that meandering river processes (cut bank erosion, point bar growth, and meander migration) can occur in ice-cemented, unvegetated permafrost environments. We find that the Onyx River's upper, single-threaded reach is meandering, and that bank cohesion is provided by ice-cemented permafrost—both on the outer banks and terraces, as well as along the point bars where ice-cemented permafrost is aggrading up through the recently-deposited bar sediments. Meander migration rates within the meandering reach are extremely close to values predicted based on observations of meander migration rates in other unvegetated rivers, however, the short (~70 day) duration of Onyx River discharge suggests these migration rates should be considered low estimates, which could be up to ~5 times higher during the actual erosion season. We find that point bar and cut bank pairs are, in some cases, roughly approaching equilibrium in terms of aggradation and erosion, preserving channel width geometry, while in other cases, rapid erosion of cut banks due to fluvial thermokarstic erosion is leading to export of bank material out of the meandering reach. In contrast, we find that sediment is largely accumulating in the braided reach of the Onyx River, where aggradation of bars within braided channels is greatly outpacing erosion from terrace margins or from within the channels. Together, these observations suggest that ice-cemented permafrost is a weak form of bank cohesion that can result in rapid landscape change in response to thermokarstic fluvial erosion, producing dynamic river channels, especially where warm meltwater encounters ice-rich permafrost deposits, and may serve as a model for interpreting the origin and climate significance of fluvial sediments on Mars.

Declaration of competing interest

The authors declare that they have no known competing financial interests or personal relationships that could have appeared to influence the work reported in this paper.

Data availability

All lidar data used in this study is available through the National Center for Airborne Laser Mapping (NCAM) and OpenTopography via: DOI: https://doi.org/10.5069/G9D50JX3. Vector mapping data produced for this study is available in the Supplementary Materials.

Acknowledgements

This work was supported in part through the U.S. National Science Foundation, Award ANT-1847067 to JSL. Any opinions, findings, and conclusions or recommendations expressed in this material are those of the authors and do not necessarily reflect the views of the National Science Foundation. Worldview satellite data provided by the Polar Geospatial Center (PGC).

Appendix A. Supplementary data

Supplementary data to this article can be found online at https://doi.org/10.1016/j.geomorph.2023.108705.

References

Babonneau, N., Savoye, B., Cremer, M., Bez, M., 2010. Sedimentary architecture in meanders of a submarine channel: detailed study of the present congo turbidite channel (Zaiango Project). J. Sediment. Res. 80 (10), 852–866. https://doi.org/10.2110/jsr.2010.078.

Black, R.F., 1982. Patterned-ground studies in Victoria Land. Antarct. J. US 17 (5), 53–54.

Bockheim, J.G., Campbell, I.B., McLeod, M., 2007. Permafrost distribution and active-layer depths in the McMurdo Dry Valleys,Antarctica. Permafr. Periglac. Process. 18 (3), 217–227. https://doi.org/10.1002/ppp.588.

Cardenas, B.T., Mohrig, D., Goudge, T.A., 2018. Fluvial stratigraphy of valley fills at Aeolis Dorsa, Mars: evidence for base-level fluctuations controlled by a downstream water body. GSA Bull. 130 (3–4), 484–498. https://doi.org/10.1130/B31567.1.

Chinn, T., Mason, P., 2016. The first 25 years of the hydrology of the Onyx River, Wright Valley, Dry Valleys,Antarctica. Polar Rec. 52 (1), 16–65. https://doi.org/10.1017/S0032247415000212.

Church, M., Ferguson, R.I., 2015. Morphodynamics: rivers beyond steady state. Water Resour. Res. 51 (4), 1883–1897. https://doi.org/10.1002/2014WR016862.

Clark, J.D., Kenyon, N.H., Pickering, K.T., 1992. Quantitative analysis of the geometry of submarine channels: implications for the classification of submarine fans. Geology 20 (7), 633–636. https://doi.org/10.1130/0091-7613(1992)020<0633:QAOTGO>2.3.CO;2.

Conovitz, P.A., McKnight, D.M., MacDonald, L.H., Fountain, A.G., House, H.R., 1998. Hydrologic processes influencing streamflow variation in Fryxell Basin, Antarctica. Retrieved from. In: Priscu, J.C. (Ed.), Ecosystem Dynamics in a Polar Desert: The McMurdo Dry Valleys, Antarctica. American Geophysical Union, pp. 93–108. http://www.agu.org/books/ar/v072/AR072p0093/AR072p0093.shtml.

Csatho, B.M., Schenk, T., Krabill, W.B., Wilson, T.J., Lyons, W.B., McKenzie, G., et al., 2005. Airborne laser scanning for high-resolution mapping of Antarctica. EOS Trans. Am. Geophys. Union 86 (25), 237–238.

Davies, N.S., Gibling, M.R., 2010. Paleozoic vegetation and the Siluro-Devonian rise of fluvial lateral accretion sets. Geology 38 (1), 51–54. https://doi.org/10.1130/G30443.1.

Doran, P.T., McKay, C.P., Clow, G.D., Dana, G.L., Fountain, A.G., Nylen, T., Lyons, W.B., 2002. Valley Floor Climate Observations From the McMurdo Dry Valleys, Antarctica, 1986–2000, 107(D24). https://doi.org/10.1029/2001JD002045.

Douglas, M.M., Li, G.K., Fischer, W.W., Rowland, J.C., Kemeny, P.C., West, A.J., et al., 2022. Organic carbon burial by river meandering partially offsets bank erosion carbon fluxes in a discontinuous permafrost floodplain. Earth Surf. Dyn. 10 (3), 421–435. https://doi.org/10.5194/esurf-10-421-2022.

Fairén, A.G., 2010. A cold and wet Mars. Icarus 208 (1), 165–175. https://doi.org/10.1016/j.icarus.2010.01.006.

Fassett, C.I., Head, J.W., 2005. Fluvial sedimentary deposits on Mars: ancient deltas in a crater lake in the Nili Fossae region. Geophys. Res. Lett. 32 (14) https://doi.org/10.1029/2005GL023456.

Fountain, A.G., Fernandez-Diaz, J., Obryk, M.K., Levy, J., Gooseff, M.N., 2017. High-resolution elevation mapping of the McMurdo Dry Valleys, Antarctica, and surrounding regions. Earth Syst. Sci. Data 9, 435–443.

Gooseff, M.N., McKnight, D.M., Doran, P.T., Lyons, W.B., 2007. Trends in Discharge and flow season timing of the Onyx River, Wright Valley, Antarctica since 1969 (No. USGS OF-2007-1047 Short Research Paper 088). U.S. Geological Survey and the National Academies.

Gooseff, Michael N., Balser, A., Bowden, W.B., Jones, J.B., 2011. Effects of hillslope thermokarst in Northern Alaska. EOS Trans. Am. Geophys. Union 90 (4), 29–30. https://doi.org/10.1029/2009EO040001.

Goudge, T.A., Fassett, C.I., Head, J.W., Mustard, J.F., Aureli, K.L., 2016. Insights into surface runoff on early Mars from paleolake basin morphology and stratigraphy. Geology 44 (6), 419–422. https://doi.org/10.1130/G37734.1.

Howard, A.D., 2009. How to make a meandering river. Proc. Natl. Acad. Sci. 106 (41), 17245–17246. https://doi.org/10.1073/pnas.0910005106.

Ielpi, A., Lapôtre, M.G.A., 2020. A tenfold slowdown in river meander migration driven by plant life. Nat. Geosci. 13 (1), 82–86. https://doi.org/10.1038/s41561-019-0491-7.

Ielpi, A., Lapôtre, M.G.A., Gibling, M.R., Boyce, C.K., 2022. The impact of vegetation on meandering rivers. Nat. Rev. Earth Environ. 3 (3), 165–178. https://doi.org/10.1038/s43017-021-00249-6.

Ielpi, A., Lapôtre, M.G.A., Finotello, A., Roy-Léveillée, P., 2023. Large sinuous rivers are slowing down in a warming Arctic. Nat. Clim. Chang. 1–7. https://doi.org/10.1038/s41558-023-01620-9.

Jarriel, T., Swartz, J., Passalacqua, P., 2021. Global rates and patterns of channel migration in river deltas. Proc. Natl. Acad. Sci. 118 (46), e2103178118 https://doi.org/10.1073/pnas.2103178118.

Karlstrom, L., Gajjar, P., Manga, M., 2013. Meander formation in supraglacial streams. J. Geophys. Res. Earth Surf. 118 (3), 1897–1907. https://doi.org/10.1002/jgrf.20135.

Lane, S.N., Richards, K.S., 1997. Linking river channel form and process: time, space and causality revisited. Earth Surf. Process. Landf. 22 (3), 249–260. https://doi.org/10.1002/(SICI)1096-9837(199703)22:3<249::AID-ESP752>3.0.CO;2-7.

Lapôtre, M.G.A., Ielpi, A., 2020. The pace of fluvial meanders on Mars and implications for the western delta deposits of Jezero Crater. AGUAdv. 1 (2), e2019AV000141 https://doi.org/10.1029/2019AV000141.

Lapôtre, M.G.A., Ielpi, A., Lamb, M.P., Williams, R.M.E., Knoll, A.H., 2019. Model for the formation of single-thread rivers in barren landscapes and implications for pre-Silurian and Martian fluvial deposits. J. Geophys. Res. Earth Surf. 124 (12), 2757–2777. https://doi.org/10.1029/2019JF005156.

Levy, J.S., Fountain, A.G., Obryk, M.K., Telling, J., Glennie, C., Pettersson, R., et al., 2018. Decadal topographic change in the McMurdo Dry Valleys of Antarctica: thermokarst subsidence, glacier thinning, and transfer of water storage from the cryosphere to the hydrosphere. Geomorphology 323, 1–18. https://doi.org/10.1016/j.geomorph.2018.09.012.

Levy, Joseph S., Fountain, A.G., Dickson, J.L., Head, J.W., Okal, M., Marchant, D.R., Watters, J., 2013. Accelerated thermokarst formation in the McMurdo Dry Valleys, Antarctica. Sci. Rep. 3 (1), 2269. https://doi.org/10.1038/srep02269.

Matsubara, Y., Howard, A.D., Burr, D.M., Williams, R.M.E., Dietrich, W.E., Moore, J.M., 2015. River meandering on Earth and Mars: a comparative study of Aeolis Dorsa meanders, Mars and possible terrestrial analogs of the Usuktuk River, AK, and the Quinn River, NV. Geomorphology 240 (C), 102–120. https://doi.org/10.1016/j.geomorph.2014.08.031.

McKnight, D.M., Niyogi, D.K., Alger, A.S., Bomblies, A., Conovitz, P.A., Tate, C.M., 1999. Dry valley streams in Antarctica: ecosystems waiting for water. Bioscience 49 (12), 985–995.

Murton, J.B., 2009. Global warming and thermokarst. In: Margesin, R. (Ed.), Permafrost Soils. Springer, Berlin, Heidelberg, pp. 185–203. https://doi.org/10.1007/978-3-540-69371-0_13.

Naito, K., Parker, G., 2020. Adjustment of self-formed bankfull channel geometry of meandering rivers: modeling study. Earth Surf. Process. Landf. 45 (13), 3313–3322. https://doi.org/10.1002/esp.4966.

Ritter, B., Diederich-Leicher, J.L., Binnie, S.A., Stuart, F.M., Wennrich, V., Bolten, A., Dunai, T.J., 2022. Impact of CaSO4-rich soil on Miocene surface preservation and Quaternary sinuous to meandering channel forms in the hyperarid Atacama Desert. Sci. Rep. 12 (1), 17951. https://doi.org/10.1038/s41598-022-22787-9.

Schumm, S.A., 1968. Speculations concerning paleohydrologic controls of terrestrial sedimentation. GSA Bull. 79 (11), 1573–1588. https://doi.org/10.1130/0016-7606(1968)79[1573:SCPCOT]2.0.CO;2.

Shaw, J., Healy, T.R., 1980. Morphology of the Onyx River system, McMurdo Sound region, Antarctica. N. Z. J. Geol. Geophys. 23 (2), 223–238. https://doi.org/10.1080/00288306.1980.10424208.

Sletten, R.S., Hallet, B., Fletcher, R.C., 2003. Resurfacing Time of Terrestrial Surfaces by the Formation and Maturation of Polygonal Patterned Ground, 108(E4). https://doi.org/10.1029/2002JE001914.

Sudman, Z., Gooseff, M.N., Fountain, A.G., Levy, J.S., Obryk, M.K., Van Horn, D., 2017. Impacts of permafrost degradation on a stream in Taylor Valley, Antarctica. Geomorphology 285 (C), 205–213. https://doi.org/10.1016/j.geomorph.2017.02.009.

Weihaupt, J.G., 1974. Possible origin and probable discharges of Meandering Channels on the planet Mars. J. Geophys. Res. 79 (14), 2073–2076. https://doi.org/10.1029/JB079i014p02073.

Wlostowski, A.N., Gooseff, M.N., McKnight, D.M., Jaros, C., Lyons, W.B., 2016. Patterns of hydrologic connectivity in the McMurdo Dry Valleys, Antarctica: a synthesis of 20 years of hydrologic data. Hydrol. Process. 30, 2958–2975. https://doi.org/10.1002/hyp.10818.

Wordsworth, R.D., 2016. The climate of early Mars. Annu. Rev. Earth Planet. Sci. 44 (1), 381–408. https://doi.org/10.1146/annurev-earth-060115-012355.

Wordsworth, R.D., Kerber, L., Pierrehumbert, R.T., Forget, F., Head, J.W., 2015. Comparison of "warm and wet" and "cold and icy" scenarios for early Mars in a 3-D climate model. J. Geophys. Res. Planets 120 (6), 1201–1219. https://doi.org/10.1002/2015JE004787.

Zhang, T., Li, D., East, A.E., Walling, D.E., Lane, S., Overeem, I., et al., 2022. Warming-driven erosion and sediment transport in cold regions. Nat. Rev. Earth Environ. 3 (12), 832–851. https://doi.org/10.1038/s43017-022-00362-0.